Dynamic knockdown of E. coli central metabolism for redirecting fluxes of primary metabolites

Citation: Brockman, Irene M., and Kristala L.J. Prather. "Dynamic Knockdown of E. Coli Central Metabolism for Redirecting Fluxes of Primary Metabolites." Metabolic Engineering 28 (March 2015): 104–113.

As Published: http://dx.doi.org/10.1016/j.ymben.2014.12.005

Publisher: Elsevier

Persistent URL: http://hdl.handle.net/1721.1/101771

Version: Author's final manuscript: final author's manuscript post peer review, without publisher's formatting or copy editing

HHS Public Access

Author manuscript

Metab Eng. Author manuscript; available in PMC 2016 March 01.

Published in final edited form as:

Metab Eng. 2015 March ; 28: 104–113. doi:10.1016/j.ymben.2014.12.005.

Dynamic knockdown of *E. coli* central metabolism for redirecting fluxes of primary metabolites

Irene M. Brockman and **Kristala L. J. Prather***

Department of Chemical Engineering Massachusetts Institute of Technology Cambridge, MA 02139, USA

Abstract

Control of native enzyme levels is important when optimizing strains for overproduction of heterologous compounds. However, for many central metabolic enzymes, static knockdown results in poor growth and protein expression. We have developed a strategy for dynamically modulating the abundance of native enzymes within the host cell and applied this to a model system for *myo*-inositol production from glucose. This system relies on controlled degradation of a key glycolytic enzyme, phosphofructokinase-I (Pfk-I). Through tuning Pfk-I levels, we have been able to develop an *E. coli* strain with a growth mode close to wild type and a production mode with an increased glucose-6-phosphate pool available for conversion into *myo*-inositol. The switch to production mode is trigged by inducer addition, allowing yield, titer, and productivity to be managed through induction time. By varying the time of Pfk-I degradation, we were able to achieve a two-fold improvement in yield and titers of *myo*-inositol.

Keywords

Metabolic flux redirection; Dynamic metabolic control; Protein degradation; Primary metabolism; Synthetic biology

1. Introduction

The introduction of heterologous enzymes into a microbial host to generate novel synthetic pathways poses a number of challenges, especially when the enzymes in those pathways compete with native enzymes for substrate. To counter this problem, common strategies utilized in rational strain design for overproduction of natural metabolites, such as gene knock-outs or promoter replacements, have typically been used (Lee et al., 2012; Tyo et al., 2010; Woolston et al., 2013). However, these approaches produce strains with only a few available control points, especially with respect to changing the cell's own metabolism

* Corresponding author: Department of Chemical Engineering, 77 Massachusetts Avenue, Room E17-504G, Cambridge, MA 02139, Phone: 617.253.1950, Fax: 617.258.5042, kljp@mit.edu.

during the course of a fermentation. The ideal flux balance for the production phase of a fermentation differs from the flux balance required at the beginning of a fermentation, when biomass production and expression of recombinant proteins are most important.

To overcome these limitations, a number of recent works have focused on experimental and theoretical advantages associated with redirecting flux in central metabolism through dynamic control of enzyme levels (Anesiadis et al., 2013; Callura et al., 2012; Farmer and Liao, 2000; Solomon et al., 2012b; Soma et al., 2014; Torella et al., 2013). While the use of inducible promoters to turn on heterologous gene expression in *E. coli* through small molecule inducers or temperature change has been well developed, methods for dynamically knocking down expression of native genes are more limited. The genetic devices developed in the context of synthetic biology offer a number of possible ways to achieve gene regulation in response to extracellular and intracellular conditions (Holtz and Keasling, 2010). However, many of these systems have been optimized on plasmids or at relatively high expression levels, making them difficult to integrate in context with heterologous biosynthetic pathways that are already taxing to the host cells (Cardinale and Arkin, 2012). Dynamic control systems which could be integrated into production strains with minimal change in baseline performance would provide a valuable advantage in microbial production of chemicals.

A potentially useful node from controlling fluxes in primary metabolism is the metabolic branch point at glucose-6-phosphate (G6P). G6P can be routed into native metabolism through both glycolysis and the oxidative pentose phosphate pathway, as well as into heterologous production of *myo*-inositol via INO1 from *Saccharomyces cerevisiae* (Hansen et al., 1999). *Myo*-inositol can be further converted into other useful products, such as glucaric acid, a biopolymer precursor (Werpy and Petersen, 2004) and *scyllo*-inositol, which has been studied as a therapeutic for Alzheimers (Yamaoka et al., 2011). The pathway for glucaric acid has already been demonstrated in *E. coli* (Moon et al., 2009) and theoretical yields of near 100% are possible; however, G6P must be directed into this pathway at the expense of central metabolism. Previous studies have focused on controlling the G6P utilization in glycolysis versus the pentose phosphate pathway (Callura et al., 2012), but dynamic redirection of G6P into a heterologous pathway has not been demonstrated. We therefore focused on control of phosphofructokinase (Pfk-I) level as a method to direct G6P into *myo*-inositol production and restrict biomass formation. Redirecting primary metabolism poses unique challenges, as heterologous pathway enzymes are often selected from secondary metabolism or may be acting on non-native substrates, while the central metabolic enzymes utilize primary metabolites very efficiently. Global studies have indicated central metabolic enzymes typically have a higher catalytic efficiency than enzymes in secondary metabolism and are likely to be operating on a substrate pool near the K_M value of the enzyme (Bar-Even et al., 2011; Bennett et al., 2009).

To minimize lag time from associated with dilution of stable proteins and generate a quick response as well as large dynamic range, we have implemented post-translational control of Pfk through use of modified SsrA tags. A number of SsrA tag variants have been reported which alter the half-life of the tagged protein or have varying degradation rates dependent on the presence and absence of SspB, an adaptor protein that tethers target proteins to

ClpXP (Andersen et al., 1998; Davis et al., 2011; McGinness et al., 2006). By appending such a tag to the coding sequencing of Pfk-I and knocking out the native copy of *sspB*, the half-life of Pfk-I can be controlled through expression of SspB from an inducible promoter. This strategy allows rapid changes in the steady-state level of Pfk-I to be achieved. Using this system in *E. coli*, we were able to achieve increases in both titer and yield of *myo*-inositol (MI), a precursor in glucaric acid production.

2. Materials and methods

2.1 Strains and plasmids

E. coli strains and plasmids used in this study are listed in Table 1. *E. coli* strain DH10B was used for molecular cloning and plasmid preparation. Production strains were constructed utilizing MG1655 *endA* (IB531) as a parent strain. Knockouts of *zwf*, *pfkB*, and *sspB* were accomplished via sequential P1 transduction from Keio collection donor strains (Baba et al., 2006). The kanamycin resistance cassette was removed after each transduction via expression of FLP recombinase from pCP20 (Datsenko and Wanner, 2000). The native *pfkA* locus was replaced with a version containing a constitutive promoter (apFAB114) and 5' UTR from the BIOFAB library (Mutalik et al., 2013) and the degradation tag AADENYSENYADAS (McGinness et al., 2006). The replacement at the *pfkA* locus was carried out via a "landing pad" method (Kuhlman and Cox, 2010). The *pfkA* coding sequence was amplified from the *E. coli* genome with primers which appended the promoter and UTR at the 5' end and the degradation tag at the 3' end of the gene. This product was cloned into the vector pTKIP-neo by restriction digest with HindIII and KpnI, yielding pTKIP-114pfkA(DAS+4). Lambda-red mediated recombination was used to introduce the tetracycline resistance marker and "landing pad" sequences amplified from pTKS/CS into the genome at the *pfkA* locus. The resultant strain was then transformed with pTKRED and pTKIP- 114pfkA(DAS+4), and integration of the construct from the pTKIP plasmid into the genome was achieved as described previously (Kuhlman and Cox, 2010). The kanamycin resistance cassette remaining after integration was cured by expression of FLP recombinase from pCP20 to yield strain IB1643.

Integration of the *tetR*-P_{LteOt}-*sspB* cassette into the genome was carried out via "clonetegration" (St-Pierre et al., 2013). The coding sequence of *sspB* was amplified from the *E. coli* genome and cloned into pKVS45 via restriction digest to yield pKVS-SspB. The vector pKVS45 includes a TetR expression cassette originally amplified from pWW308 (Solomon et al., 2012b). The entire *tetR*-P_{LtetO}-*sspB* cassette was amplified from pKVS-SspB. The pOSIP-CH backbone was also PCR amplified and cycled 10x with the *tetR*-P_{LteOt}-*sspB* fragment according to the protocol for circular polymerase extension cloning (CPEC) (Quan and Tian, 2009). The CPEC product was used to transform strain IB1643 for integration at the HK022 locus. The phage integration genes and antibiotic resistance cassette were cured with pE-FLP as described in the previously published protocol (St-Pierre et al., 2013) to yield strain IB1863.

For construction of IB1014, integration cassettes for deletion of *ptsHIcrr* and replacement of the native *galP* promoter with a strong constitutive promoter were PCR amplified from the genome of previously developed phosphotransferase system deficient (PTS-), glucose

utilizing (glucose+) strains (Solomon et al., 2012a). These cassettes contained the desired genomic deletion or promoter replacement, a kanamycin resistance cassette, and the upstream and downstream genomic homology. The PCR cassettes were sequentially integrated into IB1863 via lambda-red mediated recombination using the helper plasmid pKD46, and each kanamycin resistance cassette was cured by expression of FLP recombinase from pCP20 (Datsenko and Wanner, 2000).

During all integration steps, colonies were screened via colony PCR with OneTaq master mix. PCR amplifications for cloning or genomic integration were carried out with Q5 polymerase. Enzymes utilized for PCR amplification, restriction digests, and ligation were obtained from New England Biolabs (Ipswich, MA). Oligonucleotides were obtained from Sigma-Genosys (St. Louis, MO).

2.2 Culture medium and conditions

For plasmid preparation and genetic manipulations, strains were cultured in Luria-Bertani (LB) medium at either 30° or 37° C. Temperature sensitive plasmids were cured at 42° C.

M9 minimal medium supplemented with either 0.4% glucose or 0.4% glycerol was utilized for initial screening of promoters for *pfkA*. All additional cultures for measurement of growth and production were carried out at 30°C in a modified MOPS medium containing 10 g/L D-glucose, 3 g/L NH_4Cl, 1 g/L K_2HPO_4, 2 mM $MgSO_4$, 0.1 mM $CaCl_2$, 40 mM MOPS, 4 mM tricine, 50 mM NaCl, 100 mM Bis-Tris, 134 μM EDTA, 31 μM $FeCl_3$, 6.2 μM $ZnCl_3$, 0.76 μM $CuCl_2$, 0.42 μM $CoCl_2$, 1.62 μM H_3BO_3, and 0.081 μM $MnCl_2$. When noted, the medium was supplemented with an additional 0.2% casamino acids. For strains containing pTrc-INO1, carbenicillin (100 μg/mL) was added for plasmid maintenance. Seed cultures were initiated using a 1:100 – 1:500 dilution from LB cultures and were grown at 30°C for 18 - 24 hours in modified MOPS, until mid-exponential phase was reached. Working cultures of 50 ml in 250 ml baffled shake flasks were inoculated to OD = 0.05 from seed cultures, and for *myo*-inositol production experiments, 50 μM β-D-1-thiogalactopyranoside (IPTG) was added at inoculation. For induction of SspB in strain IB1863, anhydrotetracycline (aTc) was added at the times and concentrations indicated in the results section. Samples were taken periodically for measurement of enzyme activity, protein levels, and extracellular metabolites.

2.3 Phosphofructokinase activity assays and Western blotting

All enzymatic activity assays were carried out on crude lysates. For preparation of lysates, samples of 5-10 ml of cell culture were collected, frozen at −80°C, and then resuspended in 50 mM Tris-HCl, pH 7.4 (0.25 – 1 ml, depending on cell density). Cells were lysed via bead beating for 5 minutes and lysates clarified by centrifugation at 15,000 × g for 15 minutes. Phosphofructokinase activity was assayed using a protocol adapted from Kotlarz and Buc (Kotlarz and Buc, 1982; Kotlarz et al., 1975). The assay mixture consisted of 0.1 M Tris – HCl (pH 8.2), 10 mM $MgCl_2$, 1 mM ATP, 0.2 mM β-NADH, 1 mM fructose-6-phosphate (F6P), 1 mM NH_4Cl, 0.01% Triton X-100, 0.83 U aldolase, 0.42 U triosephosphate isomerase, and 0.42 U glycerophosphate dehydrogenase. Reaction progress was followed by measurement of absorbance at 340 nm. One unit of Pfk activity was defined as the amount

required to convert 1.0 μmole of ATP and D-fructose 6-phosphate to ADP and fructose 1,6-bisphosphate per minute at pH 8.2 and room temperature.

For Western blots to confirm disappearance of Pfk-I, lysis was carried out as for enzymatic assays. A 4-20% SDS-PAGE gel was run with 10 μg total protein per lane. Proteins were transferred from the PAGE gel to a nitrocellulose membrane and excess binding sites were blocked using 5% dry milk in TBS. The membrane was incubated at 4°C overnight with anti-Pfk-I rabbit polyclonal antibody (6.7 μg/ml) custom prepared by Genscript (Piscataway Township, NJ), rinsed, and incubated with HRP-conjugated goat anti-rabbit IgG polyclonal antibody (Santa Cruz Biotechnology, Dallas, TX) and StrepTactin-HRP (Bio-rad, Hercules, CA) at room temperature for one hour. Bands were visualized by treatment with Western blotting Luminol Reagent (Santa Cruz Biotechnology).

Total protein levels for normalization of enzymatic activities and Western blot loadings were measured using a modified Bradford assay (Zor and Selinger, 1996).

2.4 Measurement of intracellular glucose-6-phosphate and fructose-6-phosphate

Cultures of IB531, IB1863, and IB1014 were grown in triplicate in modified MOPS medium using the seed culture protocol outlined in section 2.2. Working cultures were inoculated to OD = 0.02 and incubated at 30° C. For measurement of G6P buildup after Pfk-I degradation, aTc was added to the culture one hour before collection of the cell mass.

For intracellular metabolite measurements, 20-30 ml of cells in exponential phase (OD = 0.3 – 0.9) were collected via vacuum filtration through 0.45 μM Metricel GN-6 filters (Pall, Port Washington, NY). After filtration of the culture, the filters with cell mass were immediately immersed in 10 ml of 75% ethanol solution at 80° C. The solution was vortexed for 30 seconds, incubated at 80° C for 3 minutes, and vortexed again. The filter paper was then removed and the solution centrifuged for 10 minutes at 5000 × g to remove cell debris. Incubation in boiling 75% ethanol for 3 minutes has been previously shown to result in good extraction of sugar phosphates (Gonzalez et al., 1997). The solutions were stored at −80° C until evaporation for analysis. The 75% ethanol solution was completely evaporated and the remaining solids resuspended in 200 μL water. Any solids which could not be dissolved in water were pelleted by centrifugation at 15,000 × g for 5 minutes. Enzymatic assays for G6P and F6P were carried out in 96-well plates in a Tecan infinite F200Pro plate reader (Männedorf, Switzerland). The assay solution consisted of 0.2 M triethanolamine, 0.2 mM NADP, and 5 mM $MgCl_2$ (Bergmeyer et al., 1983). After stabilization of the baseline, glucose-6-phosphate dehydrogenase was added to the assay solution and G6P levels were analyzed by following NADPH generation via fluorescence (excitation 340 nm, emission 450 nm). After complete turnover of G6P, F6P levels were analyzed by the addition phosphoglucose isomerase, which converted the remaining F6P to G6P. Intracellular metabolite levels were estimated assuming 0.4 gDCW/OD unit (Tseng et al., 2009) and an intracellular volume of 2 ml/gDCW, which would be expected for *E. coli* at a similar growth rate on glucose (Hiller et al., 2007).

2.5 Measurement of extracellular metabolites

Glucose, acetate, and *myo*-inositol levels were quantified by high performance liquid chromatography (HPLC) on an Agilent 1100 or 1200 series instrument (Santa Clara, CA) with an Aminex HPX-87H anion exchange column (300 mm by 7.8 mm; Bio-Rad Laboratories, Hercules, CA). Sulfuric acid (5 mM) at a flow rate of 0.6 mL/min was used as the mobile phase. Compounds were quantified from 10 μL sample injections using refractive index and diode array detectors. Column and refractive index detector temperatures were held at 35° C. Glucose uptake and acetate production rates were calculated using an estimated cell mass of 0.4 gDCW/OD unit (Tseng et al., 2009).

3. Results

3.1 Selection of phosphofructokinase-I as a control point for glucose-6-phosphate flux

The primary native enzymes acting on the branch point metabolite G6P are phosphoglucose isomerase (Pgi) and glucose-6-phosphate dehydrogenase (Zwf). Although knockout of these enzymes will result in a strain that cannot consume G6P (Shiue et al., submitted), they are not necessarily appropriate targets for dynamic control. The interconversion between G6P and fructose-6-phosphate (F6P) catalyzed by Pgi is near equilibrium within the cell, indicating that the enzyme may not exert significant control over flux (Stephanopoulos et al., 1998). Previous reports from *in vitro* simulation of glycolysis indicate that Pfk exerts significant control over the utilization of G6P (Delgado et al., 1993).

To better understand where control of G6P flux toward *myo*-inositol lies in this system in *E. coli*, a basic model of G6P consumption was constructed, using available *in vitro* kinetic data and published information on steady-state flux distribution, intracellular metabolite levels, and cofactor levels during growth on glucose (additional information can be found in Supplementary Tables 1 and 2). The reaction catalyzed by INO1, *myo*-inositol-1-phosphate synthase from *Saccharomyces cerevisiae*, was included as a competing reaction to generate the target heterologous compound *myo*-inositol. This initial model was used to explore inherent kinetic limitations, but did not account for changes in downstream regulation, glucose uptake rate, and cofactor pools, which occur as the levels of glycolytic enzymes are varied.

The model was used to predict steady-state rate of G6P consumption by INO1 as a function of enzyme level knockdown (Fig. 1A). 25% knockdown of Pfk is predicted to increase flux through INO1 nearly two-fold, while almost complete knockdown of Pgi would be required to achieve this increase in flux. The predicted increase in flux is also consistent with the reported K_M value of INO1, which has been estimated for G6P *in vitro* at 1.18 mM (Majumder et al., 1997). Given that intracellular G6P is predicted to be near this level, it could be expected that INO1 is not already saturated with substrate and might have capacity for increasing turnover. Based on the predicted increases in flux towards *myo*-inositol with control of Pfk levels, this enzyme was selected for further development as a control point.

3.2 Control of glucose flux and growth rate via controlled degradation of Pfk-I

With Pfk as the target for control, a strain background was developed that would allow the effect of Pfk knockdown to be cleanly observed (Fig. 2A). Pfk exists as two isozymes in *E. coli*, and the major form, Pfk-I, accounts for more than 90% of the observed activity (Keseler et al., 2011). Pfk-I was selected as the target enzyme for control, while the isozyme Pfk-II was eliminated by knockout of *pfkB*. Additionally, *zwf* was knocked out to eliminate G6P flux into the pentose phosphate pathway, generating strain IB1379. These knockouts resulted in a 13% reduction in growth rate on modified MOPS minimal medium relative to the parent strain IB531 (Supplementary Table 3).

To achieve dynamic knockdown of Pfk-I, a system based on controlled protein degradation was utilized. The coding sequence of *pfkA* was altered by appending a modified SsrA tag previously developed by McGinness *et. al.*, which results in rapid degradation of the target protein in the presence of the native *E. coli* adaptor protein SspB, but slow degradation in the absence of that protein (McGinness et al., 2006). Additionally, native regulation of Pfk-I expression was disrupted by replacement of the native promoter sequence, which contains a binding site for the transcription factor Cra, with a constitutive promoter selected from the BIOFAB modular library (Mutalik et al., 2013). Six promoters from the low range of this library were tested. All promoters showed Pfk activities higher than that observed with the wild-type for untagged Pfk, and some of the replacements resulted in growth defects, which did not correspond with Pfk activity level. The promoter selected for further testing (apFAB114) showed no growth defect after integration and had the second lowest Pfk activity among the promoters tested, although the activity was still six-fold higher than wild type (Supplementary Table 4). To make the default state “ON” (slow degradation of Pfk-I), SspB was knocked out at its native locus. Control was initially tested through aTc-inducible expression of SspB from the plasmid pKVS-SspB. This did not result in complete growth arrest in the “OFF” state, possibly due to plasmid loss or instability (data not shown). To improve system performance, the tet-expression cassette for SspB was integrated into the genome at the phage attachment site, HK022 (Fig. 2B), resulting in much better dynamic range of the system.

The resultant strain, IB1863, showed a 15% reduction in growth rate relative to IB531 on minimal medium (Fig. 3A). IB1863 and IB531 maintained similar growth profiles and no effect was seen on final OD. The baseline Pfk activity in IB1863 in the absence of induced SspB was 1.8X higher than IB531, lower than in the case of untagged Pfk-I due to low-level background degradation of Pfk-I, possibly due to leaky expression of SspB. However, upon addition of anhydrotetracycline (aTc) to induce expression of SspB from the $P_{L\text{-}tetO\text{-}1}$ promoter, Pfk-I activity in IB1863 declined very rapidly, decreasing to only 35% of wild type within one hour of SspB induction and 18% of wild type after 4 hours (Fig. 3B). The activity decline corresponded with observed growth arrest in the aTc treated flasks, which showed over 90% reduction in growth rate. The growth arrest and activity reduction were stable over the 16 hour time period tested. Some decline in Pfk activity at stationary phase can be observed in the absence of SspB induction. A portion of this may be due to leaky SspB expression. Tests with the promoter replacement alone, in the absence of inducible SspB, indicate that this can also be attributed to decreased Pfk expression from the

constitutive promoter in the stationary phase (Supplementary Table 5). Western blotting with anti-Pfk-I showed consistent levels of the protein over 16 hours in untreated IB1863, while Pfk-I levels were below the limit of detection for cultures treated with aTc (Fig. 3C). Overexpression of SspB from pKVS-SspB was also tested in a *sspB*- background in the absence of tagged Pfk-I and no change in activity was seen, confirming inducible SspB overexpression alone had no effect (Supplementary Fig. 1). These results indicate that Pfk-I degradation can be controlled through SspB induction and can be used to alter cellular phenotype.

The degree of growth arrest can be modulated through titration of inducer, allowing the entire dynamic range to be utilized, with growth rates between 0.05 hr^{-1} and 0.30 hr^{-1} at 30° C (Fig. 4). The system shows full induction at an aTc concentration of 1 ng/ml. Previous characterization of the P_{Ltet-O} promoter in a plasmid context indicated that 10 ng/ml of aTc was required for full induction (Lutz and Bujard, 1997). The relative change is likely due to differences in the amount of TetR produced through genomic versus plasmid-based expression. At a concentration of 1 ng/ml, there are 1.4×10^{15} molecules/L of aTc available in the medium. Given a biomass concentration of 10^{12} cells/L (approximately OD 1), this only provides enough aTc molecules to bind to 700 TetR molecules per cell, likely below the level produced from plasmid-based expression. The affinity of TetR for aTc is also well below the concentrations added to the medium, with the K_D for $[aTc\text{-}Mg]_2^+$ binding reported as 8×10^{-13} M (Kamionka et al., 2004).

Glucose uptake and acetate production rates were also measured in IB1863. In the ON state, IB1863 shows a profile almost identical to IB531, but as expected in the OFF state, glucose uptake is greatly reduced (Fig. 5A). Acetate production is also lower, indicative of reduced flux into lower glycolysis. Additionally, intracellular levels of glucose-6-phosphate and fructose-6-phosphate were elevated in the OFF state due to limited flux into lower glycolysis (Fig. 5B). Based on the thermodynamics of the G6P to F6P interconversion, it is expected that the sugar phosphate pool will be approximately 67% G6P and 33% F6P at equilibrium (Stephanopoulos et al., 1998). The intracellular metabolite measurements in IB1863 show a pool of 75% G6P and 25% F6P for Pfk-I knockdown and 80% G6P and 20% F6P for the control condition, consistent with the expectation that the reaction catalyzed by Pgi is near equilibrium, as discussed in the kinetic model in Section 3.1.

3.3 Application of the Pfk-I valve to *myo*-inositol production

Strains IB1863 and IB531 were transformed with pTrc-INO1, enabling IPTG-inducible expression of INO1, which catalyzes the conversion of G6P to *myo*-inositol-1-phosphate (MI1P). MI1P is then converted to MI by an endogenous phosphatase in *E. coli* (Hansen et al., 1999; Moon et al., 2009). In all cultures, INO1 expression was induced at inoculation through addition of 50 μM IPTG. Fermentations were carried out for 78 hours in shake flasks containing modified MOPS minimal medium and 10 g/L glucose. MI titers were assayed at the conclusion of the experiment. Switching of IB1863 between growth (Pfk-I ON) and production (Pfk-I OFF) modes was controlled through addition of 100 ng/ml aTc to induce SspB at t = 0, 11.5, 18, 32, and 47 hours.

Strong growth arrest was seen after induction of SspB in IB1863-I, except in the case of aTc addition at 47 hours, where the strain was in stationary phase (Fig. 6A). Activity measurements at 48 hours indicated an average 56% reduction in Pfk activity across all samples with SspB induced relative to those without SspB induction for IB1863-I and a 52% reduction in Pfk activity relative to the control strain IB531-I (Fig. 6B). The Pfk-I knockdown was quite consistent across SspB induction times, although for cultures with SspB induced at 47 hours, Pfk-I knockdown did differ between replicates, probably due to the short time available for Pfk-I degradation and the difference in relative growth phase of the replicates at that point.

Both theoretical (Anesiadis et al., 2008; Gadkar et al., 2005) and experimental studies (Solomon et al., 2012b; Soma et al., 2014) have indicated that there should be an optimal time for knockdown of a growth-coupled or essential gene within a fixed batch time to maximize product titer and yield. The theoretical work uses dynamic flux balance (dFBA) simulations to show that very early knockdown will result in the highest yields, but potentially incomplete carbon utilization within the batch, while later knockdown will result in lower yields, as more carbon is used for biomass, but faster consumption of the available substrate given the higher concentration of biocatalyst. The earliest knockdown time that allows complete consumption of glucose should then give the highest titer in the batch. The experimental work to date shows the tradeoff can be more nuanced, as very early induction of gene knockdown, while in theory delivering highest yields, can result in unexpectedly poor growth (Soma et al., 2014). As expected, MI yield and titer varied as a function of induction time, with the highest yield and titers when SspB was induced at 11.5 hours (OD = 0.5). This resulted in a more than two-fold improvement in titers due to controlled Pfk-I degradation, with 1.31 g/L MI produced with SspB induction at OD = 0.5 compared to 0.61 g/L MI without SspB induction, and a five-fold improvement over the 0.25 g/L MI observed for the parent strain IB531-I (Fig. 6C). Delaying induction of SspB beyond 11.5 hours in this 78 hour batch resulted in the expected lower yields and lower titers, as more carbon was directed into biomass formation, with yields converging to those shown in the control without SspB induction. At the other extreme, induction of SspB at inoculation resulted in lower titers due to incomplete consumption of glucose after 78 hours. However, the yield was also lower, falling outside the trend of expected higher yields at earlier SspB induction times. It was thought that this might be due to poor recombinant protein expression, but SDS-PAGE analysis indicated INO1 was expressed at levels comparable to the other conditions (Fig. 6D), so the reduced yield may be due to broader limitations in metabolic capacity when early glucose uptake is restricted. Overall, these results indicates that it is possible to improve *myo*-inositol yields and titers by delaying knockdown of Pfk-I rather than using a static knockdown strategy, and that the optimal induction time will depend on the desired batch length. Further optimization of the timing of both INO1 expression and Pfk-I knockdown could be used to minimize the time required for biomass formation and allow for the highest flux toward *myo*-inositol within the biomass formed, maximizing productivity rates.

It was noted that by 78 hours, formation of biomass had resumed even in cultures in which growth had been arrested. This corresponded with some recovery in Pfk activity, likely

indicating selection for cells that either exclude inducer or have accumulated mutations preventing the degradation of Pfk-I (Supplementary Fig. 2). While it would be most desirable to maintain full knockdown throughout the course of the fermentation, there is still a significant period of reduced activity, which provides sufficient time for flux redirection. It would be expected that having a larger proportion of cells in the culture with increased Pfk activity would hurt *myo*-inositol yield due to increased glucose utilization for biomass, but the trend shows that earlier induction of Pfk degradation, leaving the most glucose available for any "escaped" cells to consume, still resulted in higher yields and titers. As a result, we do not think that escape is driving the differences in yield and titer observed.

Analysis of lysates by SDS-PAGE showed similar expression of INO1 during exponential growth at 18 hours for IB531-I and for IB1863-I with and without SspB induction (Fig. 6D), indicating that differences in initial expression of INO1 were not a primary factor in influencing yield. At 48 hours, cultures containing IB531-I and untreated IB1863-I had reached stationary phase, and showed reduced INO1 expression, while those cultures in growth arrest after SspB induction still showed high levels of INO1 expression. Growth arrest due to dynamic Pfk-I knockdown appears to yield a metabolic state in which recombinant protein levels can still be maintained.

3.4 Application of the Pfk-I valve in a PTS- strain background

Maintaining a high glucose uptake rate is also important for maximizing MI productivity. However, uptake of glucose via the phosphotransferase system (PTS) is expected to be limited by downstream availability of phosphoenolpyruvate (PEP) when flux through Pfk-I is restricted. To test the effect of Pfk-I knockdown when glucose uptake is independent of the PTS, a PTS-glucose+ strain was generated via deletion of *ptsHIcrr* and constitutive expression of *galP*, manipulations which were previously shown to impart a PTS- glucose+ phenotype (De Anda et al., 2006; Solomon et al., 2012a). This strain, IB1014, showed a significant reduction in growth on glucose compared to IB1863, with a baseline growth rate of 0.13 hr^{-1} in glucose minimal medium at 30°C, less than half of that observed for IB1863. However, the behavior of the strain upon induction of SspB was still consistent and addition of aTc resulted in strong growth arrest, with over 90% reduction in growth rate (Fig. 7A). G6P levels were also measured in the strain without and without induction of SspB. Similar to IB1863, induction of SspB resulted in an increase in the G6P pool in IB1014 (Fig. 7B). These results indicate that the Pfk-I knockdown strategy should be applicable for G6P accumulation in a PTS- background and that the growth arrest observed in IB1863 was not dependent upon PEP limitation driving reduced glucose uptake.

IB1014 was also transformed with pTrc-INO1 to test *myo*-inositol production. In the modified MOPS minimal medium with 10 g/L glucose used for testing of IB1863-I, IB1014-I showed no growth after 36 hours when INO1 was expressed at inoculation. IB1014-I was then tested in the same base medium and with the same INO1 induction conditions, but with additional supplementation of 0.2% casamino acids. Casamino acid supplementation restored growth, although IB1014-I was still significantly impaired in growth relative to the wild type (PTS+) control IB531-I. At various time points during the fermentation in casamino acid supplemented medium, 100 ng/ml aTc was added to cultures of IB1014-I

knock down Pfk-I activity. The growth patterns observed were qualitatively similar to those seen for IB1863-I, with growth arrest occurring at initial aTc addition and eventual accumulation of biomass at long times (Supplementary Figure 3). Culture supernatant was analyzed by HPLC, but MI titers were below 0.1 g/L in IB1014-I and could not be accurately quantified. Given the poor titers, additional production experiments were not pursued in this strain. The strain could possibly be improved through adaptation on glucose or upregulation of Glk, although strong overexpression of Glk has been shown to be detrimental (Solomon et al., 2012a).

4. Discussion

In the production of MI, there is a direct competition between cellular growth and carbon flux toward product. Given this tradeoff, it is very difficult to engineer a static knockdown strategy which will not result in detrimental effects on host strain physiology, including poor growth and poor expression of recombinant proteins. To overcome this, we focused on development of a host strain that retains the positive characteristics of the parent strain with regard to growth and glucose uptake, but can be switched to a production mode with reduced carbon utilization for biomass.

Strain IB1863 was engineered to make Pfk-I the sole control point for utilization of G6P and F6P, linking cellular growth to steady-state levels of this enzyme. Through addition of an SspB-dependent degradation tag to the coding sequence of Pfk-I, the steady-state level could be controlled by expression of SspB from an inducible promoter. After these changes, IB1863 showed a modest reduction in growth rate compared to the parent strain in untreated cultures, but addition of aTc could be used to control glucose uptake, reducing growth by more than 80%. Coupling this with expression of INO1 allowed a two-fold increase in MI yield and titer to be achieved when utilizing glucose as a sole carbon source.

Notably, the greatest improvement in yield and titer came with delayed induction of SspB, indicating that the dynamic control of Pfk-I, rather than static downregulation, was necessary in order to achieve the best performance. The full extent of the system can still be explored, including combinations of different induction times and induction levels for both INO1 and SspB, allowing a variety of biomass and production tradeoffs to be tested. A particularly interesting possibility for use of this system might be in a fed-batch fermentation, where Pfk knockdown is induced after a suitable period of biomass formation and glucose is then fed at a rate matching the uptake needed for *myo*-inositol production and for minor glycolytic flux supporting cell maintenance.

Explorations of similar systems with dFBA indicate that there should be an optimal point for maximum productivity (Anesiadis et al., 2013). Given that the deletion of *pfkA* in the Δ*zwf* Δ*pfkB* background used is lethal, the productivity of a static knockout strain is zero, and dynamic control is especially appealing for this type of system. While we did not observe the direct trade-off between yield and titer predicted in the dFBA work at the batch length tested in this study, as both titer and yield increased with dynamic control in this case, productivity trends would still be important to consider, especially for a fed-batch case relying on formation of a fixed initial amount of biomass.

In addition to testing of the system in a strain relying on glucose uptake via the PTS, we also tested the applicability of Pfk-I control in a strain where glucose uptake is independent of PEP utilization. Our results showed that increases in the G6P pool could still be achieved in a PTS-background. While the particular PTS- strain examined in this study would require significant optimization to support MI production, ultimately, a strain where glucose uptake is decoupled from PEP utilization could offer the highest theoretical yields for products derived from G6P. Reducing equivalents or ATP produced within a heterologous pathway could be used to drive glucose uptake, maintaining glucose utilization even as metabolites in lower glycolysis are depleted.

In this study, we demonstrated controlled degradation of Pfk-I as a novel method for redirecting flux of G6P into a heterologous pathway. Upon addition of aTc to induce expression of SspB, Pfk-I was degraded and carbon flux into biomass was halted. This system was used to achieve improvements in both yield and titer of MI on glucose as a sole carbon source. The rapid, dynamic nature of the switching allows desirable cellular phenotypes (rapid growth, high expression of recombinant proteins) to be preserved during the growth phase of a fermentation, while still achieving reduced flux into central metabolism during the production phase. While this specific system was designed to be coupled with the first step in a pathway for glucaric acid production, it could be more broadly applied to any pathway with G6P or F6P as a branch point. This could include production of other *myo*-inositol derivatives, including *scyllo*-inositol, which has been studied for therapeutic uses (Yamaoka et al., 2011) or redirection of flux into pathways into the pentose phosphate pathway in response to cellular demand for NADPH, which is important when expressing pathways with high cofactor requirements, such as fatty acid biosynthesis.

Supplementary Material

Refer to Web version on PubMed Central for supplementary material.

Acknowledgements

This work was supported by the US National Science Foundation through the CAREER program (Grant No. CBET-0954986) and through the Biotechnology Training Program of the National Institutes of Health (I.M.B., Grant No. T32GM008334).

References

Andersen JB, Sternberg C, Poulsen LK, Bjorn SP, Givskov M, Molin S. New unstable variants of green fluorescent protein for studies of transient gene expression in bacteria. Appl Environ Microbiol. 1998; 64:2240–6. [PubMed: 9603842]

Anesiadis N, Cluett WR, Mahadevan R. Dynamic metabolic engineering for increasing bioprocess productivity. Metab Eng. 2008; 10:255–66. [PubMed: 18606241]

Anesiadis N, Kobayashi H, Cluett WR, Mahadevan R. Analysis and design of a genetic circuit for dynamic metabolic engineering. ACS Synthetic Biology. 2013

Baba T, Ara T, Hasegawa M, Takai Y, Okumura Y, Baba M, Datsenko KA, Tomita M, Wanner BL, Mori H. Construction of Escherichia coli K-12 in-frame, single-gene knockout mutants: the Keio collection. Mol Syst Biol. 2006; 2

Bar-Even A, Noor E, Savir Y, Liebermeister W, Davidi D, Tawfik DS, Milo R. The Moderately Efficient Enzyme: Evolutionary and Physicochemical Trends Shaping Enzyme Parameters. Biochemistry. 2011; 50:4402–4410. [PubMed: 21506553]

Bennett BD, Kimball EH, Gao M, Osterhout R, Van Dien SJ, Rabinowitz JD. Absolute metabolite concentrations and implied enzyme active site occupancy in Escherichia coli. Nat Chem Biol. 2009; 5:593–9. [PubMed: 19561621]

Bergmeyer, HU.; Bergmeyer, J.; Grassl, M. Methods of enzymatic analysis / editor-in-chief, Hans Ulrich Bergmeyer. 3rd ed.. Bergmeyer, Jürgen; Grassl, Marianne, editors. Verlag Chemie; Weinheim: Deerfield Beach, Fla.: 1983. p. c1983

Callura JM, Cantor CR, Collins JJ. Genetic switchboard for synthetic biology applications. Proceedings of the National Academy of Sciences of the United States of America. 2012; 109:5850–5. [PubMed: 22454498]

Cardinale S, Arkin AP. Contextualizing context for synthetic biology – identifying causes of failure of synthetic biological systems. Biotechnology Journal. 2012; 7:856–866. [PubMed: 22649052]

Datsenko KA, Wanner BL. One-step inactivation of chromosomal genes in Escherichia coli K-12 using PCR products. Proceedings of the National Academy of Sciences of the United States of America. 2000; 97:6640–5. [PubMed: 10829079]

Davis JH, Baker TA, Sauer RT. Small-Molecule Control of Protein Degradation Using Split Adaptors. ACS Chemical Biology. 2011

De Anda R, Lara AR, Hernández V, Hernández-Montalvo V, Gosset G, Bolívar F, Ramírez OT. Replacement of the glucose phosphotransferase transport system by galactose permease reduces acetate accumulation and improves process performance of Escherichia coli for recombinant protein production without impairment of growth rate. Metabolic Engineering. 2006; 8:281–290. [PubMed: 16517196]

Delgado J, Meruane J, Liao JC. Experimental determination of flux control distribution in biochemical systems: in vitro model to analyze transient metabolite concentrations. Biotechnol Bioeng. 1993; 41:1121–8. [PubMed: 18601299]

Farmer WR, Liao JC. Improving lycopene production in Escherichia coli by engineering metabolic control. Nat Biotechnol. 2000; 18:533–7. [PubMed: 10802621]

Gadkar KG, Doyle Iii FJ, Edwards JS, Mahadevan R. Estimating optimal profiles of genetic alterations using constraint-based models. Biotechnology and Bioengineering. 2005; 89:243–251. [PubMed: 15593263]

Gonzalez B, François J, Renaud M. A rapid and reliable method for metabolite extraction in yeast using boiling buffered ethanol. Yeast. 1997; 13:1347–1355. [PubMed: 9392079]

Hansen CA, Dean AB, Draths KM, Frost JW. Synthesis of 1,2,3,4-Tetrahydroxybenzene from d-Glucose:â€‰ Exploiting myo-Inositol as a Precursor to Aromatic Chemicals. Journal of the American Chemical Society. 1999; 121:3799–3800.

Hiller J, Franco-Lara E, Weuster-Botz D. Metabolic profiling of Escherichia coli cultivations: evaluation of extraction and metabolite analysis procedures. Biotechnol Lett. 2007; 29:1169–1178. [PubMed: 17479221]

Holtz WJ, Keasling JD. Engineering Static and Dynamic Control of Synthetic Pathways. Cell. 2010; 140:19–23. [PubMed: 20085699]

Kamionka A, Bogdanska-Urbaniak J, Scholz O, Hillen W. Two mutations in the tetracycline repressor change the inducer anhydrotetracycline to a corepressor. Nucleic Acids Research. 2004; 32:842–847. [PubMed: 14764926]

Keseler IM, Collado-Vides J, Santos-Zavaleta A, Peralta-Gil M, Gama-Castro S, Muñiz-Rascado L, Bonavides-Martinez C, Paley S, Krummenacker M, Altman T, Kaipa P, Spaulding A, Pacheco J, Latendresse M, Fulcher C, Sarker M, Shearer AG, Mackie A, Paulsen I, Gunsalus RP, Karp PD. EcoCyc: a comprehensive database of Escherichia coli biology. Nucleic Acids Research. 2011; 39:D583–D590. [PubMed: 21097882]

Kotlarz, D.; Buc, H. [11] Phosphofructokinases from Escherichia coli.. In: Willis, AW., editor. Methods in Enzymology. Vol. 90. Academic Press; 1982. p. 60-70.

Kotlarz D, Garreau H, Buc H. Regulation of the amount and of the activity of phosphofructokinases and pyruvate kinases in Escherichia coli. Biochimica et Biophysica Acta (BBA) -General Subjects. 1975; 381:257–268.

Kuhlman TE, Cox EC. Site-specific chromosomal integration of large synthetic constructs. Nucleic Acids Research. 2010

Lee JW, Na D, Park JM, Lee J, Choi S, Lee SY. Systems metabolic engineering of microorganisms for natural and non-natural chemicals. Nat Chem Biol. 2012; 8:536–546. [PubMed: 22596205]

Lutz R, Bujard H. Independent and tight regulation of transcriptional units in Escherichia coli via the LacR/O, the TetR/O and AraC/I1-I2 regulatory elements. Nucleic Acids Res. 1997; 25:1203–10. [PubMed: 9092630]

Majumder AL, Johnson MD, Henry SA. 1-myo-Inositol-1-phosphate synthase. Biochimica et Biophysica Acta (BBA) - Lipids and Lipid Metabolism. 1997; 1348:245–256.

McGinness KE, Baker TA, Sauer RT. Engineering controllable protein degradation. Mol Cell. 2006; 22:701–7. [PubMed: 16762842]

Moon TS, Yoon SH, Lanza AM, Roy-Mayhew JD, Prather KL. Production of glucaric acid from a synthetic pathway in recombinant Escherichia coli. Appl Environ Microbiol. 2009; 75:589–95. [PubMed: 19060162]

Mutalik VK, Guimaraes JC, Cambray G, Lam C, Christoffersen MJ, Mai Q-A, Tran AB, Paull M, Keasling JD, Arkin AP, Endy D. Precise and reliable gene expression via standard transcription and translation initiation elements. Nat Meth. 2013; 10:354–360.

Quan J, Tian J. Circular Polymerase Extension Cloning of Complex Gene Libraries and Pathways. PLoS ONE. 2009; 4:e6441. [PubMed: 19649325]

Shiue EC, Brockman IM, Prather KLJ. Improving Product Yields on D-Glucose in Escherichia coli via Alternative Carbon Sources. Biotechnol Bioeng. submitted.

Solomon KV, Moon TS, Ma B, Sanders TM, Prather KLJ. Tuning Primary Metabolism for Heterologous Pathway Productivity. ACS Synthetic Biology. 2012a

Solomon KV, Sanders TM, Prather KL. A dynamic metabolite valve for the control of central carbon metabolism. Metab Eng. 2012b; 14:661–71. [PubMed: 23026120]

Soma Y, Tsuruno K, Wada M, Yokota A, Hanai T. Metabolic flux redirection from a central metabolic pathway toward a synthetic pathway using a metabolic toggle switch. Metab Eng. 2014; 23:175–84. [PubMed: 24576819]

St-Pierre F, Cui L, Priest DG, Endy D, Dodd IB, Shearwin KE. One-Step Cloning and Chromosomal Integration of DNA. ACS Synthetic Biology. 2013

Stephanopoulos, G.; Aristidou, AA.; Nielsen, JH. Metabolic engineering : principles and methodologies. Academic Press; San Diego: 1998.

Torella JP, Ford TJ, Kim SN, Chen AM, Way JC, Silver PA. Tailored fatty acid synthesis via dynamic control of fatty acid elongation. Proceedings of the National Academy of Sciences. 2013; 110:11290–11295.

Tseng H-C, Martin CH, Nielsen DR, Prather KLJ. Metabolic Engineering of Escherichia coli for Enhanced Production of (R)- and (S)-3-Hydroxybutyrate. Applied and Environmental Microbiology. 2009; 75:3137–3145. [PubMed: 19304817]

Tyo KEJ, Kocharin K, Nielsen J. Toward design-based engineering of industrial microbes. Current Opinion in Microbiology. 2010; 13:255–262. [PubMed: 20226723]

Werpy, T.; Petersen, G. Top value added chemical from biomass, volume 1 - results of screening for potential candidates from sugars and synthetic gas. U.S. Department of Energy; Washington, D.C.: 2004.

Woolston BM, Edgar S, Stephanopoulos G. Metabolic Engineering: Past and Future. Annual Review of Chemical and Biomolecular Engineering. 2013; 4:259–288.

Yamaoka M, Osawa S, Morinaga T, Takenaka S, Yoshida K.-i. A cell factory of Bacillus subtilis engineered for the simple bioconversion of myo-inositol to scyllo inositol, a potential therapeutic agent for Alzheimer's disease. Microbial Cell Factories. 2011; 10:1–6. [PubMed: 21211066]

Zor T, Selinger Z. Linearization of the Bradford Protein Assay Increases Its Sensitivity: Theoretical and Experimental Studies. Analytical Biochemistry. 1996; 236:302–308. [PubMed: 8660509]

Highlights

- *E. coli* was engineered for inducible degradation of the glycolytic enzyme Pfk-I
- The goal was increased flux to products branching from G6P, e.g. *myo*-inositol (MI)
- The engineered strain showed increased sugar phosphate pool after Pfk-I degradation
- Dynamic Pfk-I knockdown resulted in two-fold increase in MI yield and titer

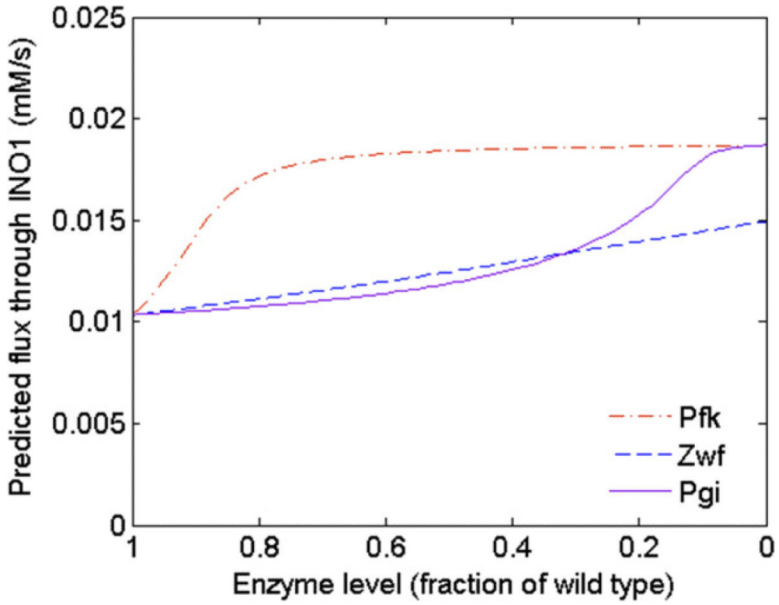

Fig. 1.

Kinetic analysis of flux through INO1. (A) Predicted changes in flux through INO1 as the levels of the native metabolic enzymes Pgi, Pfk, and Zwf are varied.

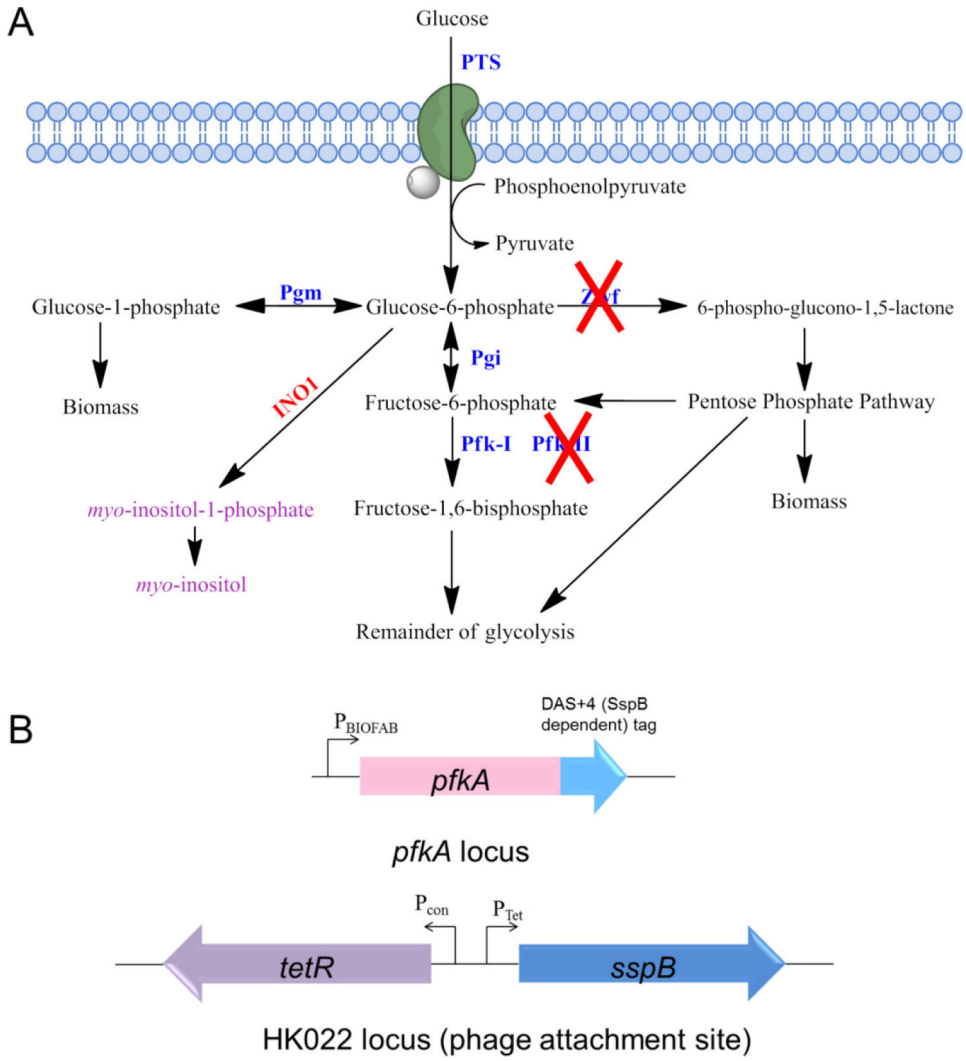

Fig. 2.

Construction of a switchable strain for *myo*-inositol production. (A) Utilization of G6P in the cell, with gene knockouts to make Pfk-I the sole control point for G6P utilization. (B) Modifications to the *pfkA* and *HK022* loci to generate aTc inducible control of Pfk-I degradation.

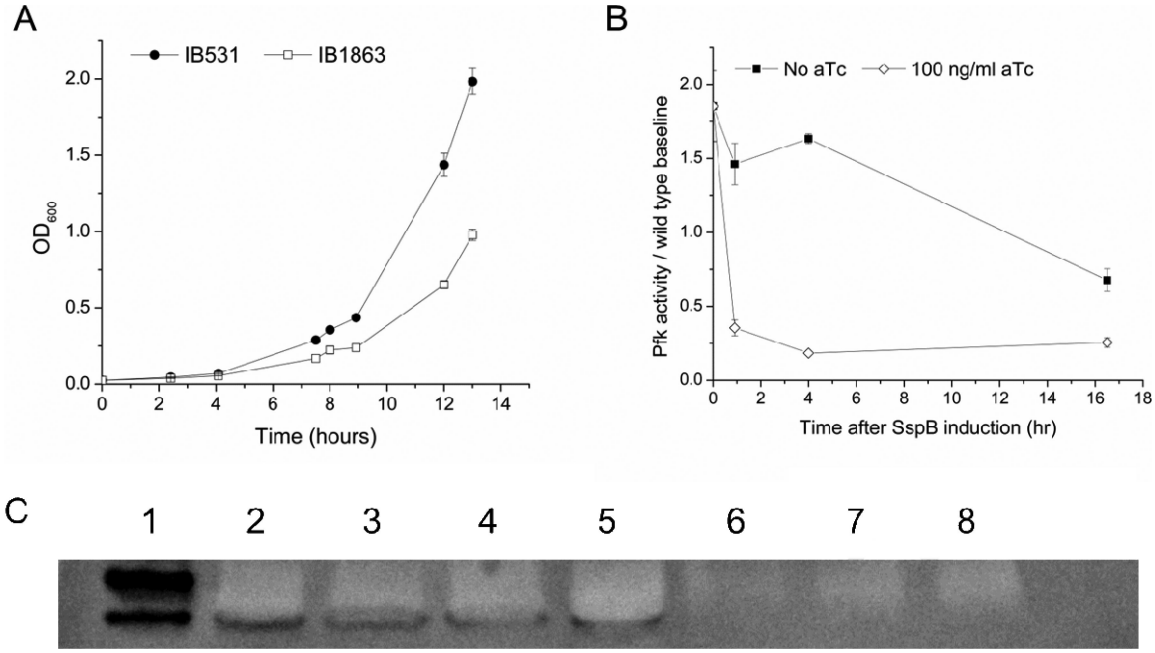

Fig. 3.

Performance of IB1863 in growth (Pfk-I ON) and production modes (Pfk-I OFF) in modified MOPS minimal medium at 30° C. (A) Baseline growth of IB1863 in comparison to parent strain IB531. (B) Decline in Pfk activity in crude lysates in response to induction of SspB with aTc. (C) Western blot confirming disappearance of Pfk-I protein from crude lysates. Lane 1: Western C ladder, lane 2: Initial culture of IB1863 before split for aTc treatment (t = 0), lanes 3 – 5: Untreated IB1863 (t = 1, 4, 16 hours), lane 6 – 8: IB1863 treated with aTc (t = 1, 4, 16, hours after treatment).

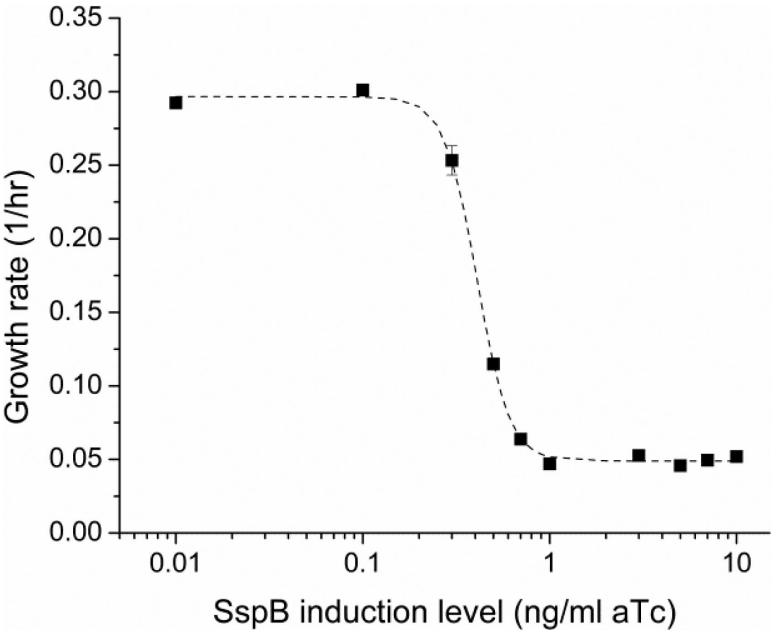

Fig. 4.

Growth rate of IB1863 as a function of aTc concentration added to the medium at inoculation. Dotted line represents fit to Hill function with n=5. All points represent triplicate mean ± SD.

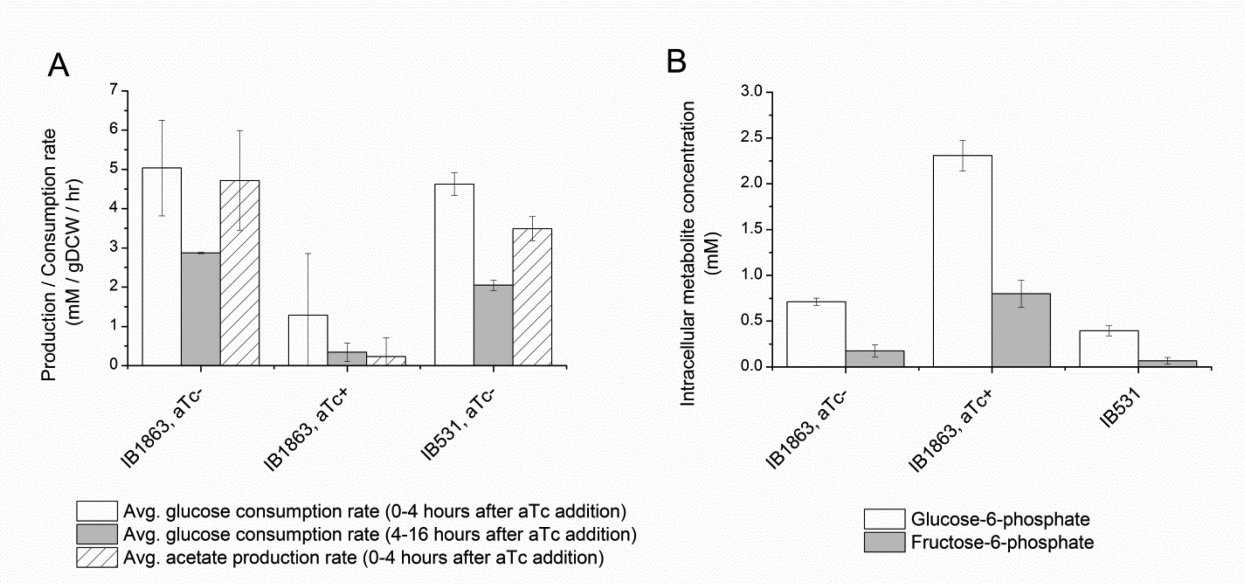

Fig. 5.

Effect of Pfk-I knockdown on carbon utilization in modified MOPS minimal medium at 30° C. (A) Glucose consumption and acetate production rates in IB1863 and IB531. Glucose consumption was measured at 4 hours and 16 hours after addition of aTc to the indicated cultures and uptake rate was averaged across the given time period. (B) Intracellular G6P and F6P pools in IB1863 and IB531. Cells were collected in exponential phase and intracellular metabolites were extracted into boiling 75% ethanol. For cultures treated with aTc, cells were collected one hour after aTc addition to the culture. Plots depict the triplicate mean ± SD.

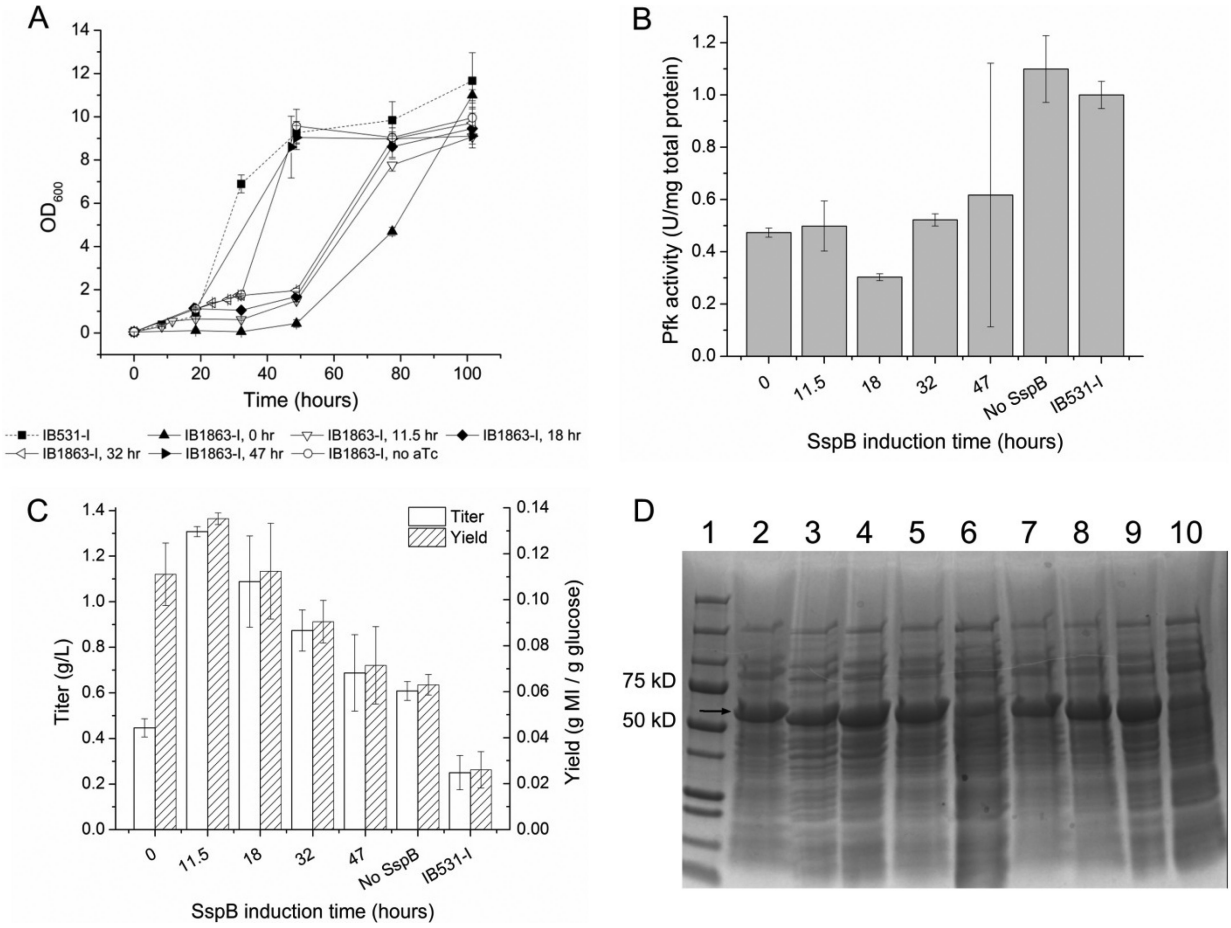

Fig. 6.

Effect of Pfk-I knockdown on MI production from glucose. (A) Growth of IB531-I and IB1863-I with aTc added at times varying from 0 to 47 hours. Points represent duplicate mean ± SD. (B) Pfk activity in all cultures at 48 hours as a function of SspB induction time. "No SspB" refers to IB1863-I without induction of SspB by aTc addition and IB531-I shows the MG1655 Δ*endA* control. (C) Yield and titer of MI at 78 hours as a function of SspB induction time in IB1863-I. (D) SDS-PAGE gel showing representative INO1 expression (indicated at arrow) in IB531-I and IB1863-I. Lane 1: ladder, lanes 2 - 5: expression at 18 hours (IB531-I, IB1863-I with aTc at t = 11.5 hours, IB1863-I with aTc at t = 18 hours, IB1863-I without aTc), lanes 6 – 10: expression at 48 hours (IB531-I, IB1863-I with aTc at t = 11.5 hours, IB1863-I with aTc at t = 18 hours, IB1863-I with aTc at t = 32 hours, IB1863-I without aTc). Plots (A) - (C) depict duplicate mean ± SD for cultures with timed SspB induction and triplicate mean ± SD for uninduced IB1863-I and IB531-I controls.

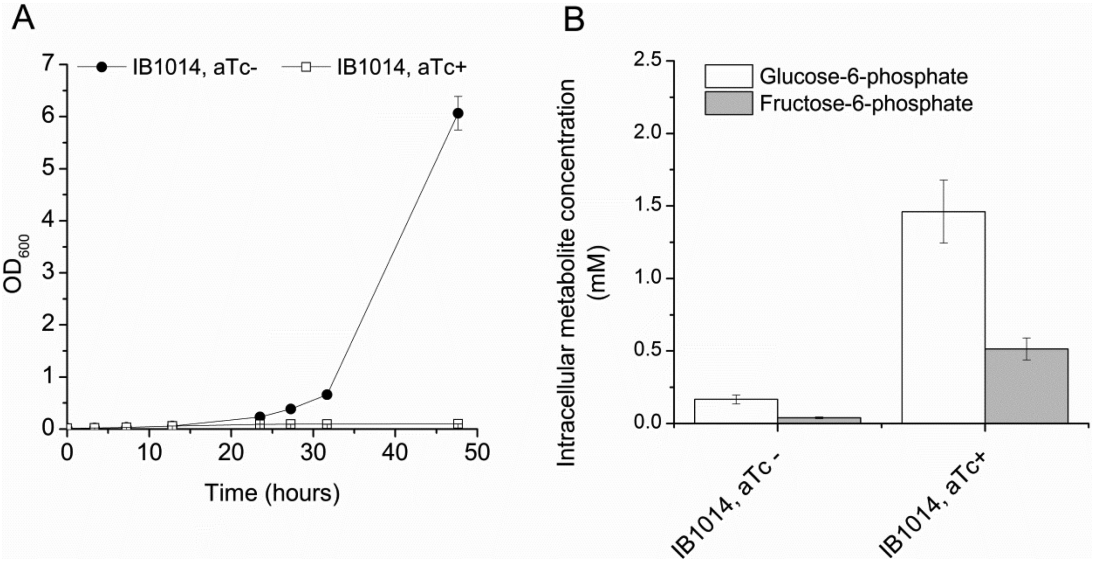

Fig. 7.

Characterization of IB1014 in modified MOPS minimal medium + 10 g/L glucose at 30° C. (A) Growth of IB1014 without aTc addition and with aTc addition at OD = 0.06. (B) Intracellular G6P and F6P pools in IB1014 with and without induction of SspB by aTc addition. Cells were collected in exponential phase and intracellular metabolites were extracted into boiling 75% ethanol. For cultures treated with aTc, cells were collected one hour after aTc addition to the culture. Plots depict the triplicate mean ± SD.

Table 1

Strains and plasmids.

Strain / plasmid	Genotype	Reference / source
Strains		
DH10B	F$^-$ *mcrA* Δ*(mrr-hsdRMS-mcrBC) ϕ80lacZ*Δ*M15* Δ*lacX74 recA1 endA1 araD139* Δ*(ara, leu)7697 galU galK λ-rpsL nupG*	Life Technologies (Carlsbad, CA)
MG1655	F$^-$ λ$^-$ *ilvG*$^-$ *frb- 50 rph-1*	ATCC #700926
IB531	MG1655 Δ*endA*	Prather Lab
IB1375	MG1655 Δ*endA* Δ*zwf*	This study
IB1379	MG1655 Δ*endA* Δ*zwf* Δ*pfkB*	This study
IB1489	MG1655 Δ*endA* Δ*zwf* Δ*pfkB* Δ*sspB*	This study
IB1643	MG1655 Δ*endA* Δ*zwf* Δ*pfkB* Δ*sspB pfkA::114-pfkA(DAS+4)*	This study
IB1863	MG1655 Δ*endA* Δ*zwf* Δ*pfkB* Δ*sspB pfkA::114-pfkA(DAS+4) HK022::tetR-Ptet-sspB*	This study
IB1014	MG1655 Δ*endA* Δ*zwf* Δ*pfkB* Δ*sspB* Δ*ptsHIcrr pfkA::114-pfkA(DAS+4) HK022::tetR-Ptet-sspB galP*^{q}	This study
IB531-I	IB531 / pTrc-INO1	This study
IB1863-I	IB1863 / pTrc-INO1	This study
IB1014-I	IB1014 / pTrc-INO1	This study
JW3197-1	F−, Δ*(araD-araB)567,* Δ*lacZ4787*(::rrnB-3), *λ*$^-$, Δ*sspB756::kan, rph-1,* Δ*(rhaD-rhaB)568, hsdR514*	(Baba et al., 2006)
JW5280-1	F−, Δ*(araD-araB)567,* Δ*lacZ4787*(::rrnB-3), *λ*$^-$, Δ*pfkB722::kan, rph-1,* Δ*(rhaD-rhaB)568, hsdR514*	(Baba et al., 2006)
JW1841-1	F−, Δ*(araD-araB)567,* Δ*lacZ4787*(::rrnB-3), *λ*$^-$, Δ*zwf-777::kan, rph-1,* Δ*(rhaD-rhaB)568, hsdR514*	(Baba et al., 2006)
Plasmids		
pCP20	Rep^a, Amp^R, Cm^R, FLP recombinase expressed by *λ* p_r under control of λ cI857	CGSC #7629
pKD46	*ori*R101, *repA* 101ts, Amp^R, *araC,* araBp-λγ-λβ-λexo	CGSC #7739
pE-FLP	*ori*R101, *repA* 101ts, Amp^R, FLP recombinase expressed by *pE*	(St-Pierre et al., 2013)
pKVS45	*p*15A, Amp^R, *tetR*, P_{Tet}	(Solomon et al., 2012b)
pKVS-SspB	pKVS45 with RBS B0034 + *E. coli* SspB inserted at the EcoRI and BamHI sites	This study
pOSIP-CH	pUC ori, RK6γ ori, Cm^R, *attP* HK022, ccdB, HK022 integrase expressed by *λ* p_r under control of λ cI857	(St-Pierre et al., 2013)
pTKIP-neo	ColE1(pBR322) *ori*, Amp^R, Kan^R	(Kuhlman and Cox, 2010)
pTKRED	*ori*R101, *repA* 101ts, Spec^R, *araC*, P_{lac} λ_γ λ_β λ_{exo} *lacI*, P_{araB} I-SceI	(Kuhlman and Cox, 2010)
pTKS/CS	*p*15A, Cm^R, P_{lacIq} *tetA*	(Kuhlman and Cox, 2010)
pTrc-INO1	pTrc99A with *S. cerevisiae* INO1 inserted at the EcoRI and HindIII sites	(Moon et al., 2009)